

UCRL-CR--104544

DE90 015910

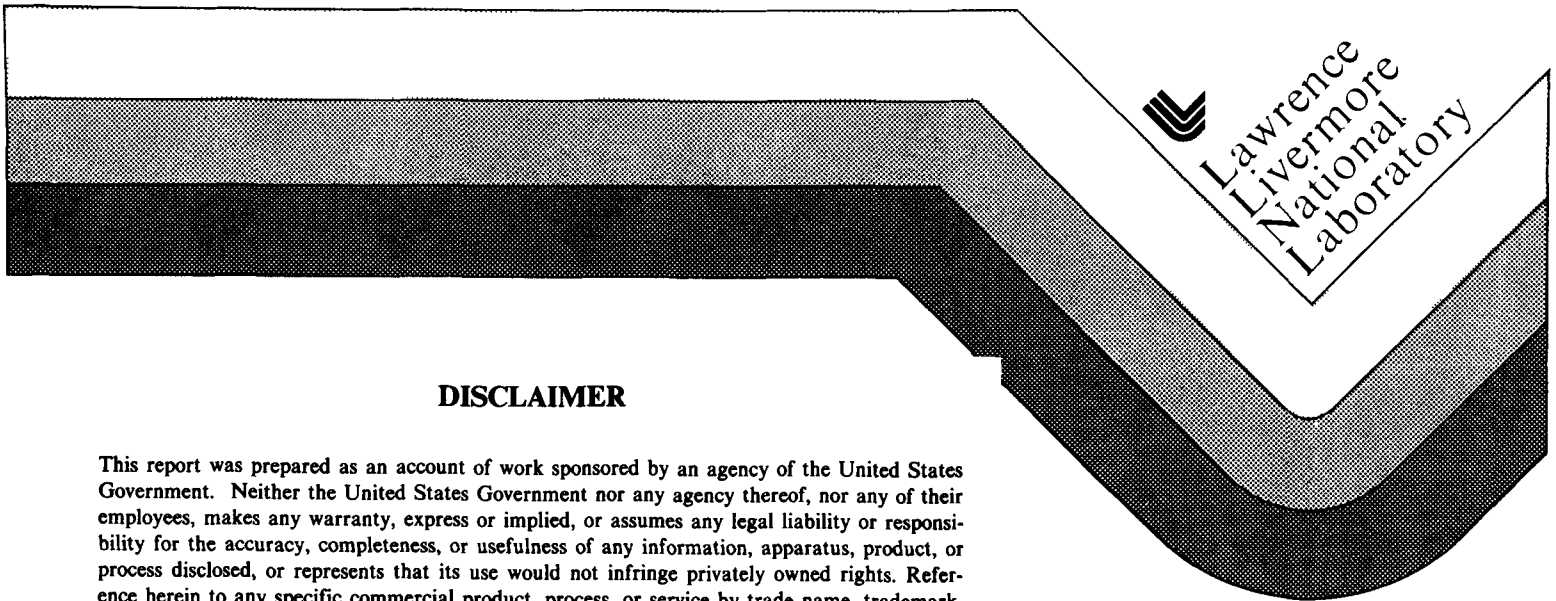
THE TRANSPORT PROPERTIES
OF ACTIVATED CARBON FIBERS

Received by OCTI

SEP 12 1990

S.L. di Vittorio
M.S. Dresselhaus
M. Endo
J-P. Issi
L. Piraux

July 1990



DISCLAIMER

This report was prepared as an account of work sponsored by an agency of the United States Government. Neither the United States Government nor any agency thereof, nor any of their employees, makes any warranty, express or implied, or assumes any legal liability or responsibility for the accuracy, completeness, or usefulness of any information, apparatus, product, or process disclosed, or represents that its use would not infringe privately owned rights. Reference herein to any specific commercial product, process, or service by trade name, trademark, manufacturer, or otherwise does not necessarily constitute or imply its endorsement, recommendation, or favoring by the United States Government or any agency thereof. The views and opinions of authors expressed herein do not necessarily state or reflect those of the United States Government or any agency thereof.

MASTER

2

DISTRIBUTION OF THIS DOCUMENT IS UNLIMITED

DISCLAIMER

This report was prepared as an account of work sponsored by an agency of the United States Government. Neither the United States Government nor any agency Thereof, nor any of their employees, makes any warranty, express or implied, or assumes any legal liability or responsibility for the accuracy, completeness, or usefulness of any information, apparatus, product, or process disclosed, or represents that its use would not infringe privately owned rights. Reference herein to any specific commercial product, process, or service by trade name, trademark, manufacturer, or otherwise does not necessarily constitute or imply its endorsement, recommendation, or favoring by the United States Government or any agency thereof. The views and opinions of authors expressed herein do not necessarily state or reflect those of the United States Government or any agency thereof.

DISCLAIMER

Portions of this document may be illegible in electronic image products. Images are produced from the best available original document.

The transport properties of activated carbon fibers.

S.L. di Vittorio

*Department of Materials Science and Engineering,
Massachusetts Institute of Technology, Cambridge, Massachusetts 02139*

M.S. Dresselhaus

*Department of Electrical Engineering and Computer Science and
Department of Physics, Massachusetts Institute of Technology,
Cambridge, Massachusetts 02139*

M. Endo

*Department of Electrical Engineering, Faculty of Engineering,
Shinshu University, Nagano 380, Japan*

J-P. Issi and L. Piraux

*Unite de Physico-Chimie et de Physique des materiaux,
Universite Catholique de Louvain, Louvain-la-Neuve, Belgium*

(Received July 24, 1990)

The transport properties of activated isotropic pitch-based carbon fibers with surface area $1000 \text{ m}^2/\text{g}$ have been investigated. We report preliminary results on the electrical conductivity, the magnetoresistance, the thermal conductivity and the thermopower of these fibers as a function of temperature. Comparisons are made to transport properties of other disordered carbons.
73.20.Fz, 73.20.Dx, 72.15.Gd

I. INTRODUCTION

Activated carbons are characterized by their extremely high porosity and high specific surface area, which can be as high as several thousands m^2/g . As a result, activated carbons are useful in applications where a large surface is required, such as filtration for anti-air pollution systems, the cleaning of drinking water and blood filtering. Another potentially far-reaching application is to use activated carbons as the electrode material of new supercapacitors.^{1,2,3}

Many techniques have been used to characterize activated carbons, such as electron microscopy⁴, X-ray scattering, and gas adsorption⁵ or mercury porosimetry.⁵ From these analyses, the pore size distribution of the material is derived, and has been classified into micropores with diameters smaller than 2 nm, mesopores with diameters between 2nm and 50 nm, and macropores larger than 50 nm. In this paper, for the first time, we characterize activated carbons using transport properties. We take advantage of the recent fabrication of activated carbon in fibrous form. Previously, activated carbon had been fabricated only in the form of grains or particles, which made quantitative transport measurements of this material impossible.

Transport properties can be used as a useful tool to characterize the activated carbon fibers (ACF). Indeed, transport properties provide a measure of the relaxation time of the carriers (whether electrical charge carriers or heat carriers), yielding information on the density as well as the nature of defects. We expect two kinds of defects in ACF: boundary scattering and scattering caused by the bulk defects related to the non-graphitic nature of the carbon material. Non-activated carbon fibers have typically a specific surface area of $10 \text{ m}^2/\text{g}$, so that boundary scattering is negligible in these fibers, but plays a significant role in ACFs. Whereas electron scattering is affected by local defects, phonons are scattered mainly by extended defects, such as dislocations, grain boundaries and other boundaries, such as pores

and surfaces. The use of the various transport experiments should therefore prove useful in analyzing the origin of scattering in the activated carbon fibers.

In this paper, we report measurements of the transport properties of a recently developed activated fiber derived from isotropic pitch, a precursor material that makes it possible to achieve higher specific surface areas (SSA) than with previously used precursor materials. The fiber studied in this paper has a SSA of $1000 \text{ m}^2/\text{g}$, which is a very high figure for any material. Indeed, in a very simple model where active carbon is described as the piling of sheets of carbon with thickness t , the SSA turns out to be $2/t\rho$, where ρ is the density of dense carbon, namely $2.25 \text{ g}/\text{cm}^3$. A SSA of $1000 \text{ m}^2/\text{g}$ yields a thickness $t=9 \text{ \AA}$. In other words, the porosity of the fiber studied in this paper corresponds to a carbon material made out of sheets of carbon 3 atoms in thickness, with the sheets separated by voids. Using 3.35 \AA as the interplanar c-axis separation, a maximum SSA of $3000 \text{ m}^2/\text{g}$ is found, which is comparable to the highest experimentally attainable SSA.

The paper is divided into four sections focusing on each of the four transport measurements carried out on the ACF: electrical conductivity, magnetoresistance, thermal conductivity and thermopower. In each section, the data are analyzed and are compared to well-studied non-graphitic carbons. When similar data were available, we have compared our results to as-grown ex-pitch fibers, in order to point out the novel features related to the high porosity. When such results could not be found, comparisons are drawn with other disordered carbons, such as glassy carbon⁶, as-grown ex-PAN fibers, or as-grown vapor-grown fibers.⁷ It should however be mentioned here that as-grown vapor-deposited fibers have a higher structural ordering than as-grown ex-pitch fibers or ex-PAN fibers.

II. FABRICATION OF ACTIVATED FIBERS

The fabrication of activated carbon fibers is a three-step process. Firstly, the fiber is formed by spinning the precursor material. Many precursor materials have been used to produce ACFs, such as phenolic materials, resins, polyacetate, cellulose, polyacrylonitrile (PAN), or pitch. In this paper, the precursor material was isotropic pitch. As a preparation for the activation process, the fiber first undergoes an anti-flamable process at a temperature of 200 to 400°C. If a structure more complicated than a fiber, such as a felt, is desired, the material can be shaped before the anti-flamable process, or alternately right afterwards. Next comes the activation process, which consists of heating the material in the temperature range 800-1200°C in the presence of CO₂ or water vapor. This process removes some carbon, through an oxidation reaction, as well as removing many impurities, and creates the highly porous structure. The main parameter that characterizes the activated carbon fibers is the specific surface area, expressed in m²/g. It is measured using the absorption isotherms of N₂ at 78K and CO₂ at 195K.

III. EXPERIMENTAL DETAILS

The samples used in these experiments consist of fibers about 1 cm long and 20 microns in diameter as determined by optical microscope measurements. In order to increase the thermal conductance of the sample, we carried out the thermal conductivity and thermopower experiments on a sample consisting of 40 fibers.

The electrical resistance of the fibers was measured under vacuum using a conventional DC four-contact technique. The typical contact resistance measured was 10 ohms. The measurements were carried out down to only 30K because of the rapidly increasing resistance at low temperature, which would have required the use of an electrometer. The magnetoresistance experiments were carried out in the field range $0 < H < 5$ tesla on a single fiber using a superconducting magnet, and

some of the results were also obtained with a conventional electromagnet.

The thermal conductivity and the thermopower of the sample were measured using the thermal potentiometer technique previously described by Piraux et al.⁸ In this technique, a four contact measurement is performed so as to eliminate the thermal contact resistances, very much in the same way as for electrical transport measurements. All leads connected to the sample were grounded on a heat sink, whose temperature was regulated so as to be the same as that of the sample, in order to minimize the heat leaks by conduction. In addition, the oven used to establish a thermal gradient along the sample was also shielded so as to reduce the losses by radiation.

The thermal properties were measured in the temperature range $55\text{K} < T < 300\text{K}$. The thermal properties were not measured in the temperature range $4.2\text{K} < T < 55\text{K}$ for two reasons: At the very lowest temperatures, where the heat capacity varies as T^3 , the thermal conductance was too small to be measurable. At intermediate temperatures, the time needed to reach thermal equilibrium is inversely proportional to the conductance, and thus was extremely long.

IV. EXPERIMENTAL RESULTS

Electrical conductivity:

The temperature dependence of the electrical conductivity is shown in Fig. 1. The magnitude of the room temperature resistivity ($2 \times 10^{-3} \Omega\cdot\text{m}$) is higher than that of any other pristine fiber. For comparison, we extracted from ref.⁷ the resistivity of an ex-pitch fiber heat-treated to 1000°C , which is the range of temperature used for the activation process ($800^\circ\text{C} < T_{HT} < 1200^\circ\text{C}$). Although we used the result given for ex-mesophase pitch, since no data were available for isotropic pitch, the large difference in resistivity ($7 \times 10^{-5} \Omega\cdot\text{m}$ vs. $2 \times 10^{-3} \Omega\cdot\text{m}$) proves that the high porosity

plays a major role in determining the electrical properties. In such a highly resistive material, a very important question is whether the material is homogeneous, and whether the current is carried by the bulk of the fiber, instead of, say, a thin surface layer. Based on TEM pictures, the structure of the surface of the fiber looks very similar to the bulk, so that we are indeed measuring the bulk resistivity of the fiber.⁹ As the temperature is lowered, the resistivity increases steeply, which is very similar to the behavior in glassy carbon. This behavior is also observed in ex-PAN and ex-pitch fibers with $T_{HT} < 1000^{\circ}\text{C}$, but not in benzene-derived fibers which have a nearly flat resistivity in the low to room temperature range, characteristic of a better structural ordering.

Depending on the temperature and the amount of disorder in the material, we expect various laws to govern the temperature dependence of the resistivity. The precursor pitch material has been heat-treated to temperatures of $800^{\circ}\text{C} < T_{HT} < 1200^{\circ}\text{C}$, so that the original organic molecules have been destroyed and our material is made essentially out of carbon. As demonstrated by the predominantly positive room temperature thermopower S , the high density of defects results in a predominantly p-type material, with a large density of holes. The chemisorption of other chemical species, mainly oxygen, on the huge surface of the activated carbon fiber is another possible mechanism for charge transfer. As opposed to pristine graphite or turbostratic graphite, we do not have a semimetal or a nearly-compensated semiconductor. The right electronic model for activated carbon is a density of states populated with a large density of holes, with the states at the Fermi level however localized because of the high porosity-induced disorder.

Within this model, several competing mechanisms can account for the temperature-dependent resistivity. At high temperature, thermal excitation of electrons from the Fermi level to the mobility edge will populate some extended states,

although the disorder is so high in ACFs that it is possible that all states are localized, and that there does not exist a mobility edge. At lower temperature, thermal excitation is unlikely and transport occurs through an electron variable-range hopping mechanism¹⁰. When both mechanisms are taken into account, the following law for the electrical conductivity is obtained:

$$\sigma = \sigma_0 \exp\left[-\left(\frac{T}{T_0}\right)^{-n}\right] + \sigma_1 \exp\left[-\left(\frac{\epsilon_1}{kT}\right)\right] \quad (1)$$

where σ_0 and σ_1 , are the conductivities at infinite temperature for the two processes considered, T_0 is a temperature related to the localization length, and ϵ_1 the energy difference between the mobility edge and the Fermi level. The first term in Eq. 1 is the variable-range hopping term, whereas the last term describes thermal excitation to the mobility edge. The variable n depends on the dimensionality of the transport, as well as on the amount of electron-electron correlation. We will find a small value for the localization length in the next paragraph, so that coulombic correlation might play an important role. Sometimes, several terms representing thermal excitation can exist in one formula, describing the thermal activation of electrons to various kinds of defects in the material. Such a law was used by Endo et al. to fit the conductivity of carbon blacks in ref.¹¹. For the sake of completeness, we should also mention the model used by Baker and Bragg¹² for glassy carbon. This model has a 1D weak localization component, which the authors associate with small ribbons of carbon existing in glassy carbon. Due to the difference in microstructure between glassy carbon and activated carbon, the Baker and Bragg model, as expected, was not found to provide a good fit to the resistivity data for the ACFs and can thus be ruled out.

In this paper, the experimental temperature-dependent conductivity will be fitted

to the first term of Eq. 1. The microstructure of activated carbons as observed using TEM by Huttepain et al.⁴ indicates a structure formed of crumpled carbon sheets. Activated carbon is described as made up of continuous stacks of aromatic layers very distorted and entangled, and with very high radii of curvature. This is an indication that transport in activated carbons is two-dimensional, so that we will use the exponent $n=1/3$ in Eq. 1. This $1/3$ exponent is also found to provide the best fit to the experimental data among the three $1/2$, $1/3$ and $1/4$ exponents, corresponding respectively to 1D, 2D and 3D variable range hopping. Experimentally, it is found that the second term in Eq. 1 is not necessary to obtain a good fit to the data in Fig. 1. This is consistent with the very large disorder present in the fibers: the mobility edge is much higher in energy than the Fermi level or may not even exist, so that thermal excitations can be neglected. On Fig.1, the experimental results are shown as triangles, and the solid line is the theoretical fit. From the fit, we extract values $\sigma_0 = 1.97 \times 10^4 (\Omega.m)^{-1}$ and $T_0 = 1.27 \times 10^4$ K. Following Mott¹⁰, we obtain an estimate for the localization length in activated carbon fibers using the formula:

$$\xi = \sqrt{\frac{27}{\pi N(E_F) k T_0}} \quad (2)$$

where $N(E_F)$ is the density of states at the Fermi level. We use the value of T_0 extracted from the conductivity data, and a density of states corresponding to pristine graphite away from the band edge, which is approximately linear in the energy. Following ref.⁷, we use the formula for the density of states:

$$N(E) = \frac{8|E|}{3\pi a_0^2 \gamma_0^2} \quad (3)$$

where a_0 is the in plane lattice constant of graphite $a_0 = 2.462 \text{ \AA}$, and γ_0 is the nearest neighbor overlap energy, whose value is $\gamma_0 = 3.16 \pm 0.05 \text{ eV}$.⁷ As indicated

by the small value of the thermopower, the carrier density is large, owing to the large concentration of defects in the material. For the present calculation, we will choose a carrier concentration of 1 carrier per 10^2 carbon atoms, as compared to one carrier per 10^4 atoms in graphite. This value is quite arbitrary, but it is not critical since the localization length depends only weakly on the carrier density (as the fourth root actually). We thus find an estimate for the localization length $\xi=20$ Å which is on the same order as the average distance between pores.⁹ This is an indication that the localization phenomenon is induced by the random potential created by the presence of pores in the material, or by the presence of dangling bonds. More conclusive results could be obtained by correlating the localization length with the average distance between pores for several activated fibers with a large range of specific areas. In the particular fiber studied in this paper, the average distance between pores is approximately equal to the average pore radius. With increasing specific surface area, however, the average pore dimension remains roughly constant, whereas the density of pores increases, thus the average distance between pores is expected to decrease, and we therefore expect the localization length to decrease with increasing specific surface area.

Magnetoresistance:

We also performed transverse magnetoresistance measurements in the field range $0 < H < 5$ tesla at various temperatures, as shown in Fig. 2. The magnetoresistance is weak and positive, increasing in magnitude with decreasing temperature. This behavior is a general feature of highly disordered carbons, such as ex-PAN and ex-pitch fibers, but also glassy carbon.^{7,13} As readily seen from the temperature dependence of the conductivity, the transport properties of ACF cannot be understood within the framework of band theory, and the positive magnetoresistance does not correspond to the conventional quadratic increase in field $\rho(H) = \rho(0) \times [1 + (\mu H)^2]$

with $n=2$. As of now, the origin of this positive magnetoresistance is however not well understood. A power law fit of the magnetoresistance curves yield exponents consistently in the $n=1.3$ to $n=1.8$ range. For very disordered ex-PAN fibers, Hambourger¹⁴ showed that the magnetoresistance was nearly isotropic. In light of this result, a comparison of the longitudinal and transverse magnetoresistance would be instructive. Indeed, recent theories on magnetoresistance in the variable-range hopping regime¹⁵ predict a quadratic increase in the resistivity at low fields, and a saturation at higher fields for materials in the variable-range hopping regime far away from the metal-insulator transition. Their theory however predicts a vanishing longitudinal magnetoresistance, as opposed to the result of ref. ¹⁴

Thermal conductivity:

The temperature dependence of the thermal conductance is shown in Fig. 3. The curve from 85K to 300K is dominated by a T^3 type law. This law is characteristic of thermal conduction by radiation during the experiment. It is not an intrinsic property of the material, but is found whenever the thermal conductance of the sample is dominated by the radiative exchanges between the parts of the measuring apparatus, which are not all at the same temperature. At lower temperatures, the curve deviates substantially from the T^3 curve. In order to estimate an order of magnitude for the thermal conductivity in the 55K to liquid nitrogen temperature range, we have fitted the curve to a T^3 law between 100K and 300K and we have then subtracted this value from the conductance at low temperature. This fit is shown as the dotted line on the curve. It can be seen on the insert to fig. 3, which shows a log-log plot of the temperature dependence of the thermal conductance, that the measured conductance deviates substantially from a straight line at low temperature. We therefore estimate an upper limit for the thermal conductivity of the fibers around liquid nitrogen temperature of 0.25 W/m.K, which is more than a factor of 5 lower

than for as-grown ex-PAN fibers.¹⁶ This result also proves that boundary scattering plays a major role in the scattering of phonons as well as in electron scattering in activated carbon fibers, as expected. Using the Wiedemann-Franz relationship, we find an estimate for the electronic contribution to the thermal conductivity of 10^{-4} W/m.K. Thus we conclude that the heat in these materials is carried by phonons, and that electrons hardly play any role in heat transport.

Thermopower:

The curve for the temperature-dependence of the thermopower S between 55K and room temperature is displayed in Fig. 4. Because of the low thermal conductance of the fibers, the thermopower is very difficult to measure, and we estimate an error-bar of $\pm 0.2\mu V/K$, substantially higher than the estimated error for better conducting materials. The thermopower of ACF, as shown in Fig. 4, is weakly positive above 150K and weakly negative below this temperature. At much lower temperatures, we expect the magnitude of the thermopower to decrease, since $S=0$ at $T=0K$. The general behavior for $S(T)$ in Fig. 4 is very similar to that found by Endo et al.¹⁹ for as-grown benzene-derived carbon fibers, which show a positive thermopower for temperatures above 140K and weakly negative below, with an empirically linear region from 50K to room temperature. Their result is added to Fig. 4 as a dashed line for comparison. This result proves that conduction in ACFs at room temperature is hole-dominated, similar to other disordered carbon structures¹⁶, whereas mixed carrier conduction takes place at low temperatures. The small magnitude of S indicates that the carrier density is large, although localized. This last result is consistent with the large density of dangling bonds associated with the pores. The weak negative thermopower at low temperatures is similar to the result found by Endo et al.¹⁹ in as-grown vapor-deposited fibers, and was then attributed to a donor behavior of the iron spheres used to catalyze the growth

from the vapor phase. It is not clear as of now if this negative thermopower at low temperatures is a general feature of disordered carbons.

V. CONCLUSION

Preliminary measurements of the electrical and thermal transport properties of activated carbon fibers with surface area $1000\text{m}^2/\text{g}$ have been reported. As expected from the large surface area, boundary scattering is very strong and the activated fibers are found to be very resistive, both electrically and thermally. We have shown that the porosity plays a very important role in determining the thermal and electrical transport properties. Quantitative studies are needed where the effect of disorder in the carbon material can be separated from the effect of the large surface area. As stated above, all measurements in this paper were performed in vacuum. Also of interest would be the study of the electrical properties of activated carbon fibers as a function of the amount of gas adsorbed or trapped in the pores and also the chemical species of the adsorbates because of the high density of dangling bonds in the activated carbon fibers. Since thermal measurements have to be carried out in a vacuum, thermal transport studies in adsorbed fibers would be very difficult. With regard to the electrical transport, we have witnessed a change on the order of a few percent when measuring the electrical resistivity of the fibers in air relative to vacuum.

VI. ACKNOWLEDGEMENTS

We would like to thank Dr. G. Dresselhaus for many stimulating discussions. We gratefully acknowledge support in part by a grant from the Lawrence Livermore National Laboratory.

- ¹M. Endo, Y. Okada and H. Nakamura, Synth. Metals 34, 739 (1989)
- ²I. Tanahashi, A. Yoshida and A. Nishina, Carbon 28, 477 (1990)
- ³A. Yoshida, I. Tanahashi, Y. Takeuchi and A. Nishino, IEEE Transactions on components, hybrids and manufacturing technology, CHMT-10 1, 100(1987)
- ⁴M. Huttepain and A. Oberlin, Carbon 28, 103 (1990)
- ⁵R.P. Bansal, J-B. Donnet and F. Stoeckli, Active Carbon, Marcel Dekker, New York (1988)
- ⁶G.M. Jenkins and K. Kawamura, Nature 231, 175 (1971)
- ⁷M.S. Dresselhaus, G. Dresselhaus, K. Sugihara, I.L. Spain and H.A. Goldberg, Graphite Fibers and Filaments, Springer-Verlag (1988)
- ⁸L. Piraux, J-P. Issi and P. Coopmans, Measurement, 5, 2 (1987)
- ⁹M. Endo, private communication
- ¹⁰N. Mott, Conduction in non-crystalline materials, Clarendon Press, Oxford(1987)
- ¹¹M. Endo, A. Kato, H. Ueno and M. Shiraishi, Transaction of the Institute of Electrical Engineers of Japan, 108-A, No.7, 279 (1988)
- ¹²Dennis F. Baker and Robert H. Bragg, Phys. Rev. B28, 2219 (1983)
- ¹³D. Robson, F.Y.I. Assabghy, E.G. Cooper and D.J.E Ingram, J. Phys. D6, 1822(1973)
- ¹⁴P.D. Hambourger, Appl. Phys. Comm. 5, 223(1986)
- ¹⁵U. Sivan, O. Entin-Wohlmann and Y.Imry, Phys. Rev. Letters 60, 1566 (1988)
- ¹⁶J. Heremans and C.P. Beetz Jr, Phys. Rev. B32, 1981 (1985)

¹⁷O.K. Griffith and R.L. Gayley, Carbon 3,541(1966)

¹⁸A.A. Bright, Phys. Rev. B20, 5142(1979)

¹⁹M. Endo, I. Tamagawa and T. Koyama, Jpn. J. of Appl. Phys. 16, 1771 (1977)

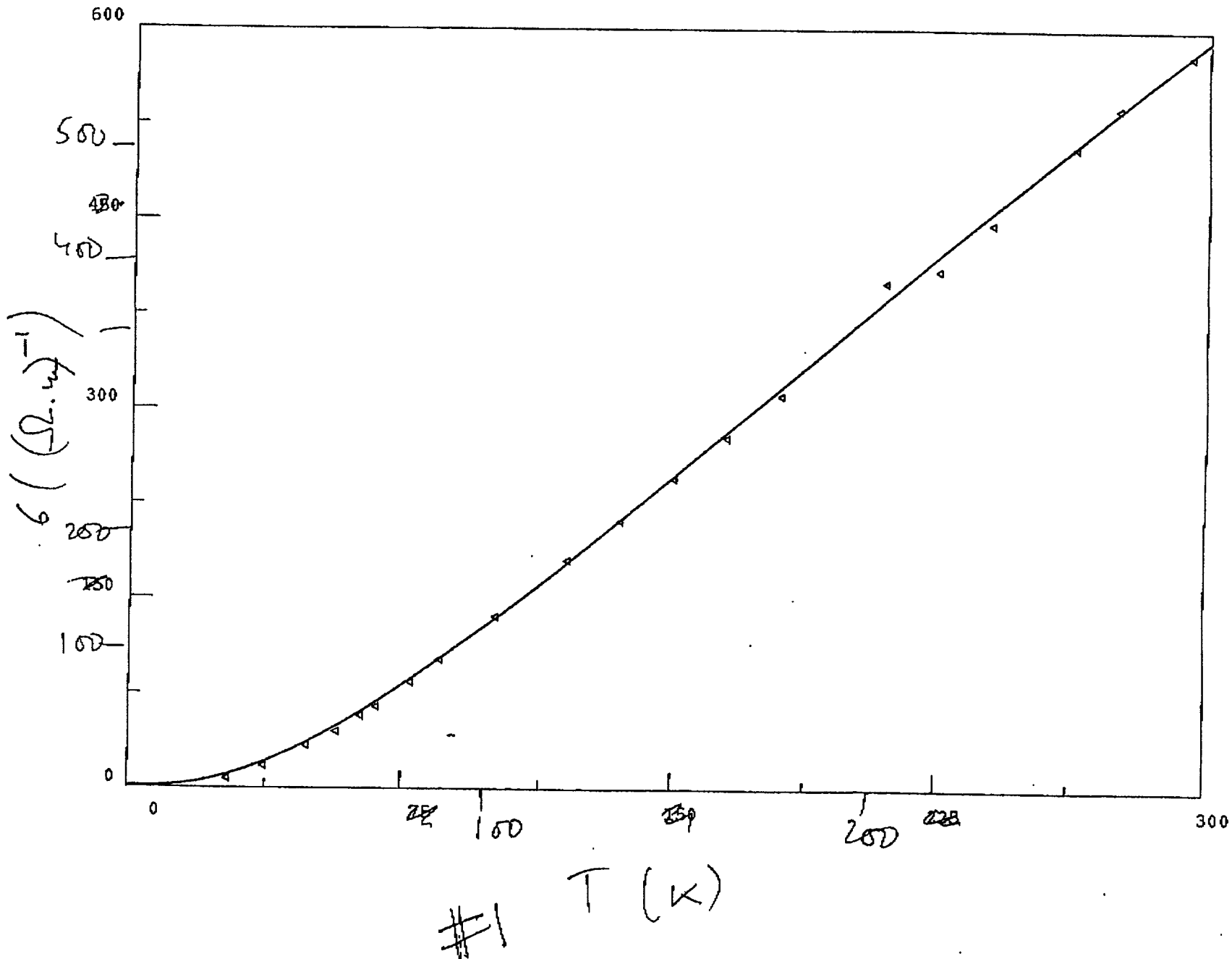
VII. FIGURES CAPTIONS

FIG. 1. The temperature dependence of the conductivity from 20K to room temperature for an activated carbon fiber. The dotted line shows the fit to a 2D variable-range hopping model.

FIG. 2. The magnetoresistance of activated carbon fibers from 0 to 5 tesla in the temperature range 27K to liquid nitrogen temperature. Note the positive sign of the magnetoresistance.

FIG. 3. The temperature dependence of the thermal conductance between 55K and room temperature. The same data are plotted on a log-log scale in the insert, which shows the temperature range where radiative transport is dominant over conductive transport.

FIG. 4. The temperature dependence of the thermopower in the temperature range 55K to room temperature. The dashed line represents the result of ref. 19 for as-grown vapor-deposited carbon fibers.



~~Magnetoresistance at various temperatures~~

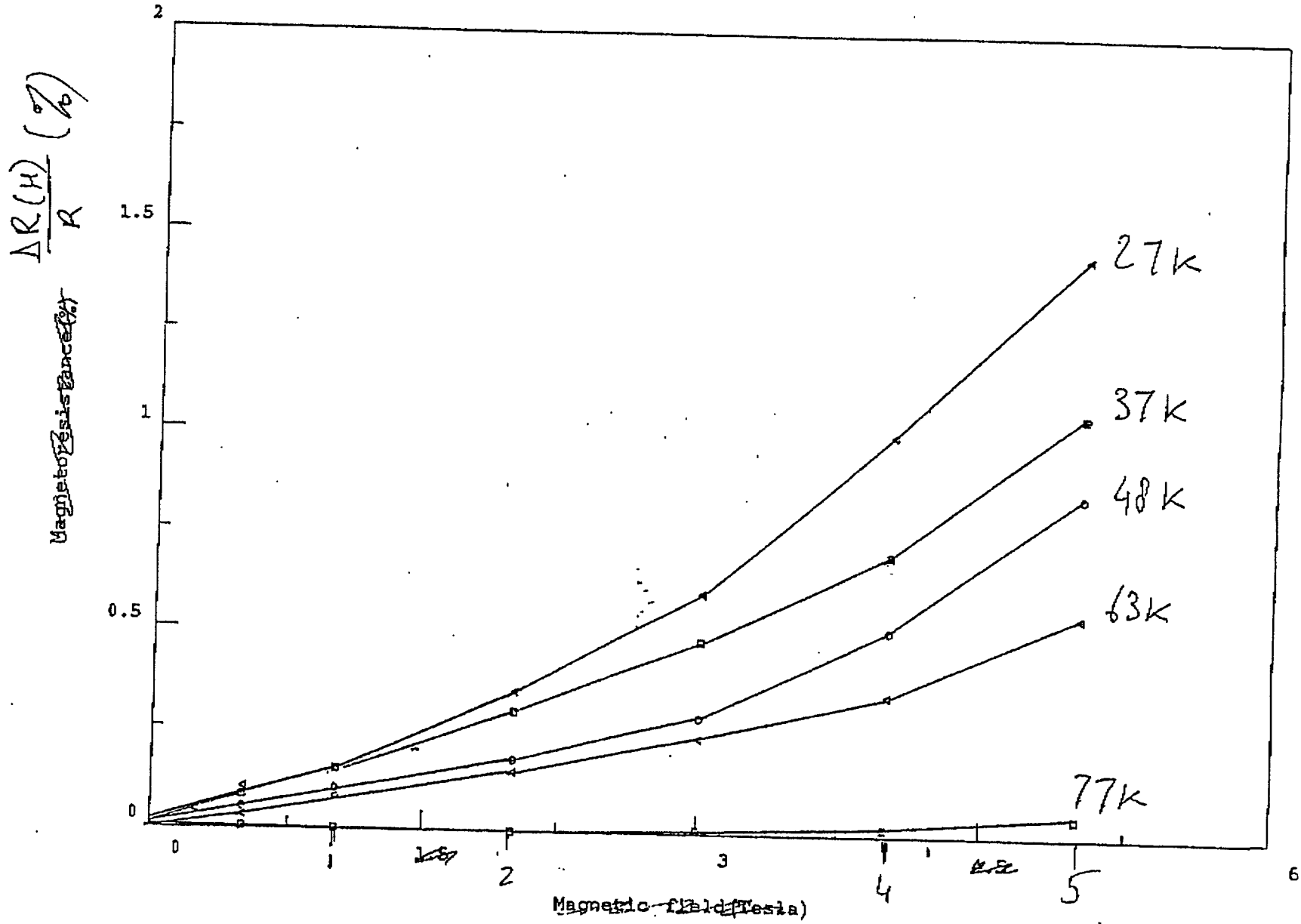
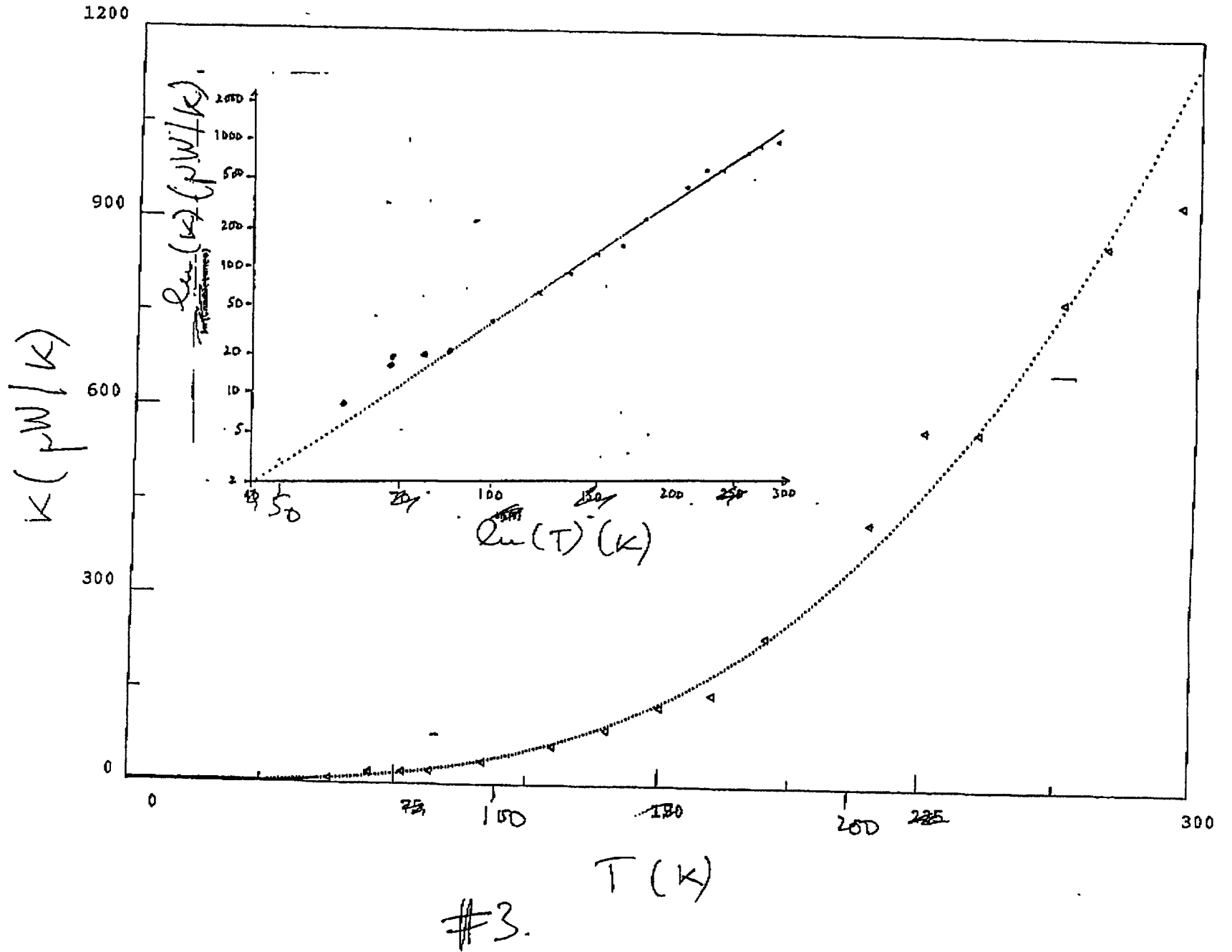
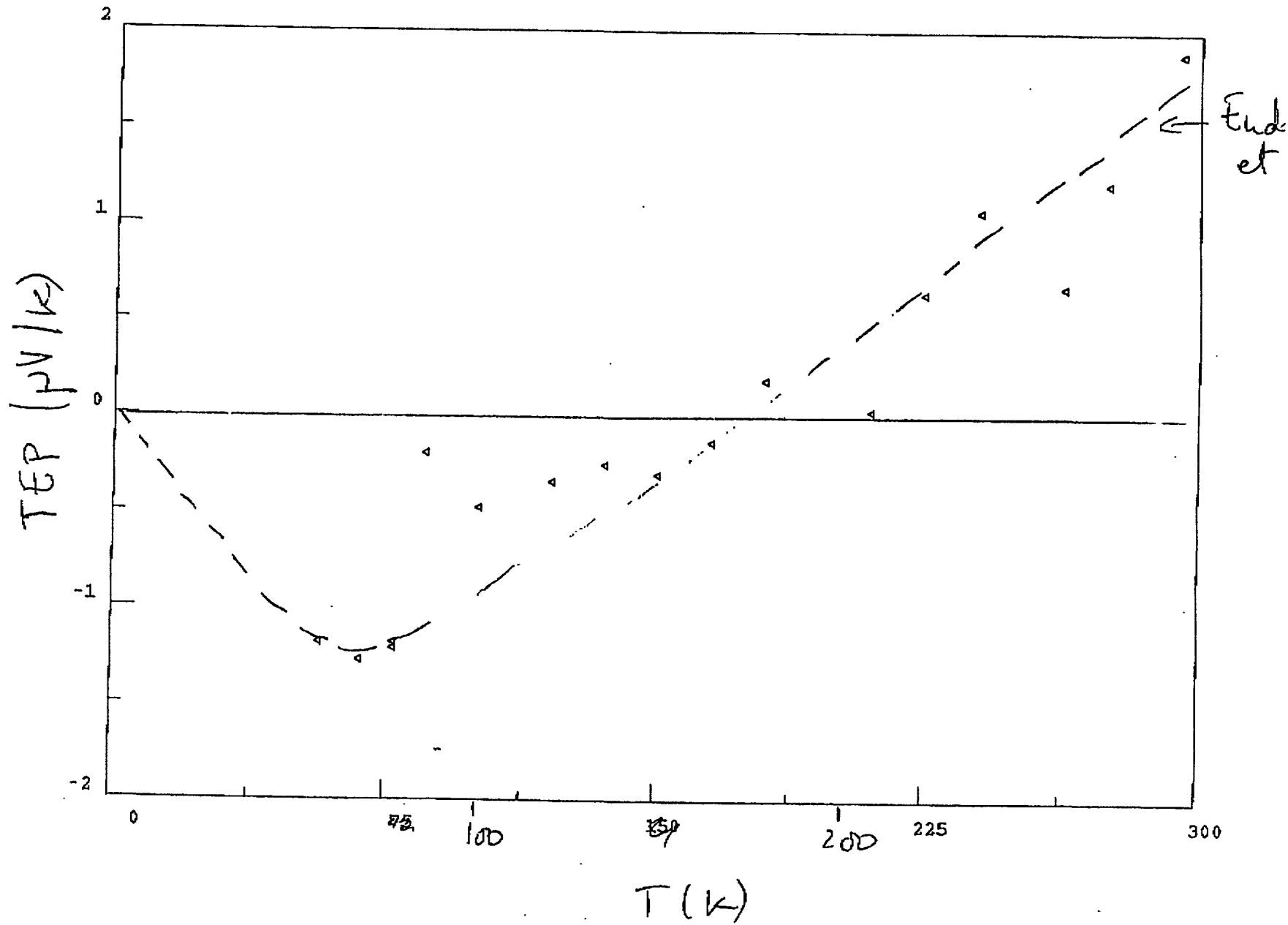


Fig 2 H (tesla).





#4

Technical Information Department · Lawrence Livermore National Laboratory
University of California · Livermore, California 94551

